Phys. Rev. Lett. **71**, 1222–1229 (1993). For an extensive discussion of BEC in many different systems, see *Bose-Einstein Condensation*, edited by A. Griffin, D. Snoke, and S. Stringari (Cambridge U.P., Cambridge, 1995).

[7]See the following volumes for numerous articles and references on the subjects of laser cooling and trapping. N. R. Newbury and C. E. Wieman, "Resource Letter TNA-1: Trapping of neutral atoms," Am. J. Phys. **64**, 18–20 (1996) (this article also provides extensive references on magnetic trapping); C. Wieman and S. Chu, (Eds.), *Special Issue on Laser Trapping and Cooling*, J. Opt. Soc. Am. B **6** (11) (1989); *Proceedings, Enrico Fermi International Summer School on Laser Manipulation of Atoms and Ions, Varenna, Italy*, edited by E. Arimondo, W. Phillips, and F. Strumia (North-Holland, Amsterdam, 1992).

[8]For review of the hydrogen work, see T. Greytak, in *Bose-Einstein Condensation*, edited by A. Griffin, D. Snoke, and S. Stringari (Cambridge U.P., Cambridge, 1995), p. 131.

[9]E. Raab, M. Prentiss, A. Cable, S. Chu, and D. E. Pritchard, "Trapping of neutral sodium atoms with radiation pressure," Phys. Rev. Lett. **59**, 2631–2634 (1987).

[10]C. Monroe, W. Swann, H. Robinson, and C. Wieman, "Very cold trapped atoms in a vapor cell," Phys. Rev. Lett. **65**, 1571–1574 (1990).

[11]M. H. Anderson, W. Petrich, J. R. Ensher, and E. A. Cornell, "Reduction of light-assisted collisional loss rate from a low-pressure vapor cell trap," Phys. Rev. A **50**, R3597–3600 (1994); "High densities of cold atoms in a dark spontaneous-force optical trap," W. Ketterle, K. B. Davis, M. A. Joffe, A. Martin, and D. E. Pritchard, Phys. Rev. Lett. **70**, 2253 (1993).

[12]D. Sesko, T. Walker, C. Monroe, A. Gallagher, and C. Wieman, "Collisional losses from a light force atom trap," Phys. Rev. Lett. **63**, 961–964 (1989); T. Walker, D. Sesko, and C. Wieman, "Collective behavior of optically trapped neutral atoms," Phys. Rev. Lett. **64**, 408–411 (1990); D. Sesko, T. Walker, and C. Wieman, "Behavior of neutral atoms in a spontaneous force trap," J. Opt. Soc. Am. B **8**, 946–958 (1991).

[13]N. Petrich, M. H. Anderson, J. R. Ensher, and E. A. Cornell, "Behavior of atoms in a compressed magneto-optical trap," J. Opt. Soc. Am. B **11**, 1332–1335 (1994).

[14]W. Petrich, M. H. Anderson, J. R. Ensher, and E. A. Cornell, "Stable tightly confining magnetic trap for evaporative cooling of neutral atoms," Phys. Rev. Lett. **74**, 3352–3355 (1995).

[15]D. E. Pritchard, K. Helmerson, and A. G. Martin, "Atom traps," in *Proceedings of the 11th International Conference on Atomic Physics*, edited by S. Haroche, J. C. Gay, and G. Grynberg (World Scientific, Singapore, 1989), pp. 179–197.

[16]M. Holland and J. Cooper, "Expansion of a Bose-Einstein condensate in a harmonic potential," Phys. Rev. A **53**, R1954–1957 (1996).

[17]K. B. Davis, M. O. Mewes, N. J. vanDruten, D. S. Durfee, D. M. Dvrn, and W. Ketterle, "Bose Einstein condensation in a gas of sodium atoms," Phys. Rev. Lett. **75**, 3969 (1995).

Surface charges on circuit wires and resistors play three roles

J. D. Jackson
University of California at Berkeley, Berkeley, California 94720-7300

(Received 11 September 1995; accepted 1 November 1995)

The significance of the surface electric charge densities associated with current-carrying circuits is often not appreciated. In general, the conductors of a current-carrying circuit must have nonuniform surface charge densities on them (1) to maintain the potential around the circuit, (2) to provide the electric field in the space outside the conductors, and (3) to assure the confined flow of current. The surface charges and associated electric field can vary greatly, depending on the location and orientation of other parts of the circuit. We illustrate these ideas with a circuit consisting of a resistor and a battery connected by wires and other conductors, in a geometry that permits solution with a Fourier–Bessel series, while giving flexibility in choice of wire and resistor sizes and location of the battery. Plots of the Poynting vector graphically demonstrate energy flow from the battery to the resistive elements. For a resistor with a large resistance, the potentials and surface charge densities around the current-carrying circuit are nearly the same as for the open circuit with the resistor removed. For such resistors, the capacitance of a resistor and its adjacent elements, defined in terms of the surface and interface charges present while current flows, is roughly the same as the capacitance of the adjacent elements of the open circuit alone. The discussion is in terms of time-independent currents and voltages, but applies also to low-frequency ac circuits. © *1996 American Association of Physics Teachers.*

I. INTRODUCTION

The ideas of electric charges and potentials of conducting surfaces in electrostatics on the one hand and current flow in simple circuits on the other are disjoint topics in almost all elementary physics textbooks. Such texts usually begin electricity and magnetism with electrostatics—first, point charges, then conducting surfaces at different potentials, surface charge densities, etc. To segue into magnetism (and to treat a practical topic), the texts then discuss current flow in simple circuits—wires, resistors, batteries. Currents are described as charges in motion within the interior of the elements of the circuit, but the charges are rapidly subsumed into current densities or total currents obeying Ohm's law. In electrostatics, charges are always stationary; in circuits, charges are always in motion.

A cursory inspection of some beginning undergraduate texts[1–10] in the Berkeley Physics Library showed that only one (the new book by Chabay and Sherwood[1]) mentioned surface charges on the wires or resistors. In some, a figure showing a battery in the circuit has plus and minus signs next to the battery plates, but it is not clear whether this is a hint at charges present or only an indication of the sign of the potential at the terminals of the battery. If a text discusses the charging of a capacitor, charges do surface again on the plates of the capacitor, but there is no mention of stationary charge elsewhere on the circuit. With the early notable exception of Jefimenko's book,[11] intermediate,[12–14] or advanced texts[15–18] are no better. My book does not even treat circuits, except in a few problems associated with capacitance or inductance. It is very true that the amounts of charge

on the wires in a circuit are generally small—the capacitance per unit length of an ordinary lamp cord is measured in picofarads per meter—but they are significant, nonetheless.

Over the years the pages of this journal and a few books have contained discussions of one or another aspect of the electric fields or stationary surface charges associated with current-carrying conductors or simple circuits.[19–30] Already mentioned are the books by Jefimenko[11] and Chabay and Sherwood.[1] The correct analytic solution for the special case of a uniform straight cylindrical wire with a cylindrically symmetric return path and remote battery appeared 63 years ago in a book by Schaefer,[19] and was published independently 50 or more years ago by Marcus[20] and by Sommerfeld.[21] Notable at the qualitative level are the classroom demonstrations of the electric fields and charges accompanying circuits by Jefimenko,[22] Parker,[26] and Moreau *et al.*[29] Some of the discussion focuses on what makes a current flow, especially what makes it turn a corner when a wire is bent.[23–25] That there are localized accumulations of surface charge to assure that the current does not escape from the wire is made clear—"... when the current is steady it is 'guided' along the conducting wire,";[23] "... this linear variation of the charge distribution [for a system of long straight wires] does indeed produce uniform axial electric fields within the conductor surfaces."[24]

Unfortunately, the discussions are too qualitative or incomplete or so specialized as to omit what I believe are equally important aspects of the surface charges, those of maintaining the potential around a circuit and providing the electric field throughout space. It is a truism that the electromagnetics of a circuit is ultimately determined by the disposition of all the charges—in the wires as current, on the surfaces as stationary charge densities, and within the battery or other source of emf.[31] Nevertheless, statements such as (describing a simple circuit of switch, wires, resistor, and battery), "Surface charges are set up immediately after the switch is closed and the resulting electric fields drive current in the circuit," mislead in that the surface charge densities can be vastly different on a given part of the circuit, for the same current flow, depending on the location of the rest of the components. Furthermore, for a circuit in which the resistor has a very different resistance from the low-resistance wires connecting it, there is localization of charge at each end of the resistor that is similar to the charge present if current flow is stopped by removal of the resistor. This fact demonstrates that the surface charge densities play multiple roles in keeping the current confined and maintaining the potential and fields in and around the circuit.

What do we offer beyond the previous literature? The treatments of the long straight wire,[19–21] or localized configurations of such wires[24] illustrate nicely the presence of surface charge densities on current-carrying circuit elements, but do not eliminate all the apparent confusion. Our contribution is a generalization of the long wire of uniform conductivity connected to a remote battery. The discussion closest to ours is that of Heald,[27] who treats a heterogeneous circuit in two dimensions—an infinitely long circular cylinder of negligible wall thickness, whose wall has zero resistivity, except over an angular range $\theta=\pm\alpha$ (region of the resistor), and a battery across $\theta=\pm\pi$.

We consider the circuit shown in Fig. 1. The azimuthally symmetric geometry is retained, as is the straight central conductor of uniform circular cross section of radius a,[32] now of finite length. The conductor is not uniform, however,

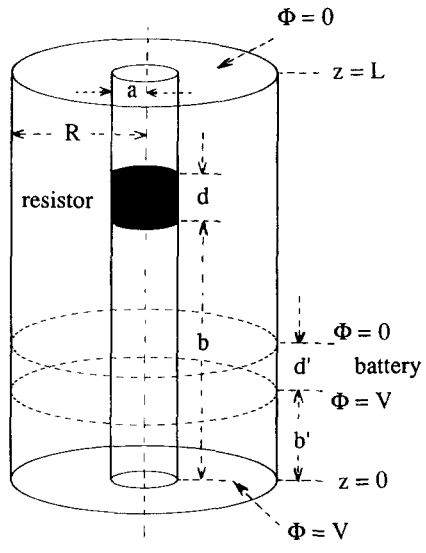

Fig. 1. Sketch of the circuit of wires, resistor, and battery. A central circular column of radius a and length L consists of two wires, one of length b and the other of length $(L-b-d)$, with a cylindrical resistor of radius a and length d between (shaded region). The wires have resistivity ρ_0, the resistor, ρ_1. The column is terminated by two flat concentric circular plates of radius R and zero resistivity. The circuit is completed by a hollow cylindrical battery cage such that the potential on the bottom plate and for a distance $z=b'$ up the cage is V. The potential falls linearly to zero at $z=b'+d'$, and is zero beyond and on the top plate. The region, $z=b'$ to $z=b'+d'$ is the battery. When the resistor is in place, current flows up the central column. The voltage drop along the column is determined by the ratio of resistivities (and b and d). When the resistor is absent, the bottom plate and wire are at potential V, while the top plate and wire are at zero potential.

but consists of wires (resistivity ρ_0) on either side of a resistor (resistivity ρ_1). The total length of the central column is L; the resistor is of length d; the bottom wire is of length b; the top wire is of length $(L-b-d)$. The circuit is completed by circular plates of radius R at $z=0$ and $z=L$, and a cylindrical battery cage at $\rho=R$, $0<z<L$. The plates are assumed to have zero resistivity and so are equipotentials. The return part of the circuit at $\rho=R$ is such that the electrostatic potential there is $\Phi(R,z)=V$ for $0\leqslant z\leqslant b'$, $\Phi(R,z)=V[1-(z-b')/d']$ for $b'<z\leqslant b'+d'$ and $\Phi(R,z)=0$ for $b'+d'<z\leqslant L$. In the limit of $d'\to 0$, the potential at $\rho=R$ is that of a localized ring battery at $z=b'$. In the limit $b'\to 0$, $d'\to L$, there is a uniform potential drop from $z=0$ to $z=L$, akin to the outer cage of a cylindrical time projection chamber, a particle physics detector.[33] The cylindrical geometry and azimuthal symmetry permits solution of the boundary value problem for the potential in terms of modified Bessel functions of order zero in ρ and trigonometric functions in z, with arbitrary choices of all parameters. The details of the solution are given in Appendix A.

Another generalization is our consideration of the comparison electrostatic problem that occurs when the resistor is removed. A relaxation technique is used to obtain numerical solutions. For simplicity of computation, we restrict our comparisons to examples of centrally located (in z) resistors and either a centrally located battery ($d'\approx 0$, $b'=L/2$) or a uniform potential drop ($b'=0$, $d'=L$). The relaxation grid spans one half of the circuit shown in Fig. 1, namely, $0\leqslant z/L\leqslant 0.5$ $(0\leqslant i\leqslant M)$ and $0\leqslant\rho\leqslant R$ $(0\leqslant j\leqslant N)$, with $M\leqslant 40$, $N\leqslant 60$. For the "open circuit" examples given, the charge densities for $z>L/2$ are the negatives of those at $z'=L-z$ and the potentials possess an obvious symmetry, modulo a

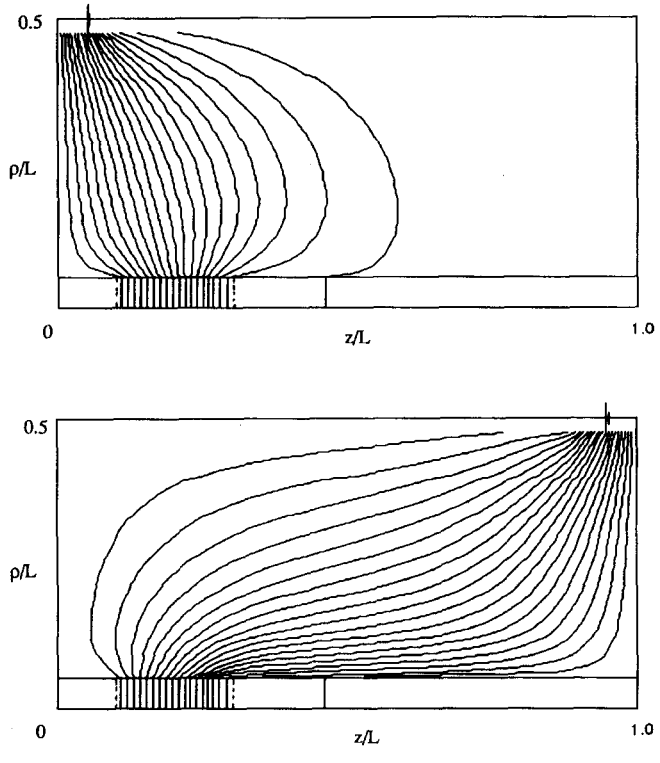

Fig. 2. Equipotential contours for a resistor of length $d/L=0.2$, located between $b/L=0.1$ and $(b+d)/L=0.3$, and a ring battery $(d'=0)$ at $b'/L=0.05$ (top) and $b'/L=0.95$ (bottom). The contours (left to right) are $\Phi/V=0.95$ (0.05) 0.05. The other circuit parameters are column radius $a/L=0.05$, outer cylinder radius $R/L=0.5$, resistivity ratio $r=50$. Dotted lines mark the ends of the resistor.

constant. Details of the two-dimensional relaxation method for cylindrical coordinates (ρ,z), including the method of handling the region containing the z axis $(\rho=0)$, are given in Appendix B.

While our discussion is phrased in terms of steady-state currents and voltages, the considerations are applicable to low-frequency alternating currents. The range of applicability is for frequencies ω such that $\omega\tau_1\ll 1$ and $\omega\tau_2\ll 1$, where $\tau_{1,2}$ are the inductive and capacitive relaxation times, $\tau_1=\mathscr{L}/\mathscr{R}$ and $\tau_2=\mathscr{R}C$. [We are forced into somewhat unconventional symbols for inductance and resistance by our previous use of L and R as lengths!] At frequencies satisfying these conditions the fields and charges oscillate in step with the voltage, without phase lag or lead. The steady-state language may be interpreted as instantaneous in time, everywhere around the circuit.

The range of validity of the quasistatic approximation can be explored as follows. First of all, electrostatics is predicated on $\nabla\times\mathbf{E}=0$, but in fact $\nabla\times\mathbf{E}=-\partial\mathbf{B}/\partial t$. In the quasistatic limit, a current $I(t)$ in the central column produces an azimuthal magnetic induction, $B_\phi(t)=\mu_0 I(t)\rho/2\pi a^2$ for $0<\rho<a$, and $B_\phi(t)=\mu_0 I(t)/2\pi\rho$ for $\rho>a$. The time-varying flux produces an additional axial electric field at $\rho=a$ of magnitude $|\Delta E_z|=\mu_0\omega I/4\pi$, as can be seen from the integral form of Faraday's law with an appropriate path in the ρ–z plane. The electrostatic axial electric field varies along the central column, but its order of magnitude is $|E_z|=O(V/L)$. Putting $V=I\mathscr{R}$ and requiring that the electrostatic electric field be very large compared to $|\Delta E_z|$, we find the criterion of approximate validity of the electrostatic description of the electric fields to be

$$\mathscr{R}\gg\mathscr{R}_c,\quad \text{where } \mathscr{R}_c=\frac{\mu_0}{4\pi}\omega L=377\frac{L}{2\lambda}\ \text{ohms}.$$

Here λ is the free-space wavelength associated with the frequency ω. The inductance of the circuit of Fig. 1 is approximately, $\mathscr{L}\approx(\mu_0/4\pi)L\ln(R^2/a^2)$, neglecting the contribution from the interior of the central column. The putative criterion, $\omega\tau_1\ll 1$, can be tested:

$$\omega\tau_1=\frac{\omega\mathscr{L}}{\mathscr{R}}\ll\frac{\omega\mathscr{L}}{\mathscr{R}_c}\approx\ln(R^2/a^2).$$

Since the final expression is of order unity, the condition on the resistance $\mathscr{R}$ assures that $\omega\tau_1\ll 1$.

We show below that the capacitance of the circuit of Fig. 1 is of the order $C=O(4\pi\epsilon_0 a_{\text{eff}})$, with $a_{\text{eff}}=a+R^2/4L$, the first contribution from the surface charges on the column and the second from the charge on the annular plates. The criterion $\omega\tau_2\ll 1$ implies that $4\pi\epsilon_0\omega a_{\text{eff}}\mathscr{R}\ll 1$. But the "electrostatics" criterion requires

$$\omega\tau_2=O(4\pi\epsilon_0\omega a_{\text{eff}}\mathscr{R})\gg 4\pi\epsilon_0\omega a_{\text{eff}}\mathscr{R}_c=4\pi^2\frac{a_{\text{eff}}L}{\lambda^2}.$$

The joint conditions

$$4\pi^2\frac{a_{\text{eff}}L}{\lambda^2}\ll\omega\tau_2\ll 1,$$

can surely be satisfied for long enough wavelengths. With $a=1$ cm and $L=R=10$ cm, the lower end of the inequality is $(\nu/\nu_0)^2$ with $\nu_0\approx 0.8$ GHz, while $\mathscr{R}_c\approx 51\ \nu/\nu_0$ ohms.

To complete the discussion, consider the requirement of legitimate neglect of Maxwell's displacement current. The current density is of the order $|J|=O(I/\pi a^2)$ while the displacement current is of the order of $|\partial\mathbf{D}/\partial t|=O(\omega\epsilon_0 V/L)=O(\omega\epsilon_0 I\mathscr{R}/L)$. The static approximation for the magnetic field is thus valid provided

$$\mathscr{R}\ll 377\frac{\lambda L}{2\pi^2 a^2}\ \text{ohms}.$$

We note in passing that when the resistance equals its upper bound, $\omega\tau_2=O(4La_{\text{eff}}/a^2)$, a number somewhat larger than unity. Like $\omega\tau_2$, the resistance is bracketed between two bounds,

$$377\frac{L}{2\lambda}\ll\mathscr{R}\ll 377\frac{\lambda L}{2\pi^2 a^2}\ \text{ohms}.$$

It is easy to see that the bracketing criteria for $\omega\tau_2$ and $\mathscr{R}$ fail at roughly the same frequency, to wit, when the wavelength is no longer very large compared with the dimensions of the circuit.

For the reader with little interest in the details, we summarize the rather obvious conclusions. For simplicity, consider a circuit consisting of a resistor connected by wires to a battery (or low-frequency ac source). Assume that the resistance of the resistor is large compared to the internal resistance of the battery and that of the wires. The circuit is opened and closed by removing and inserting the resistor (think of screwing in a light bulb), with the wires and battery otherwise undisturbed. When the circuit is open, charge is distributed along the surfaces of the wires in such a manner that the potential on each wire is constant and the same as at the corresponding terminal of the battery. At the end of each wire, where the resistor would be, there is a larger accumulation of charge, opposite in sign, one from the other, to

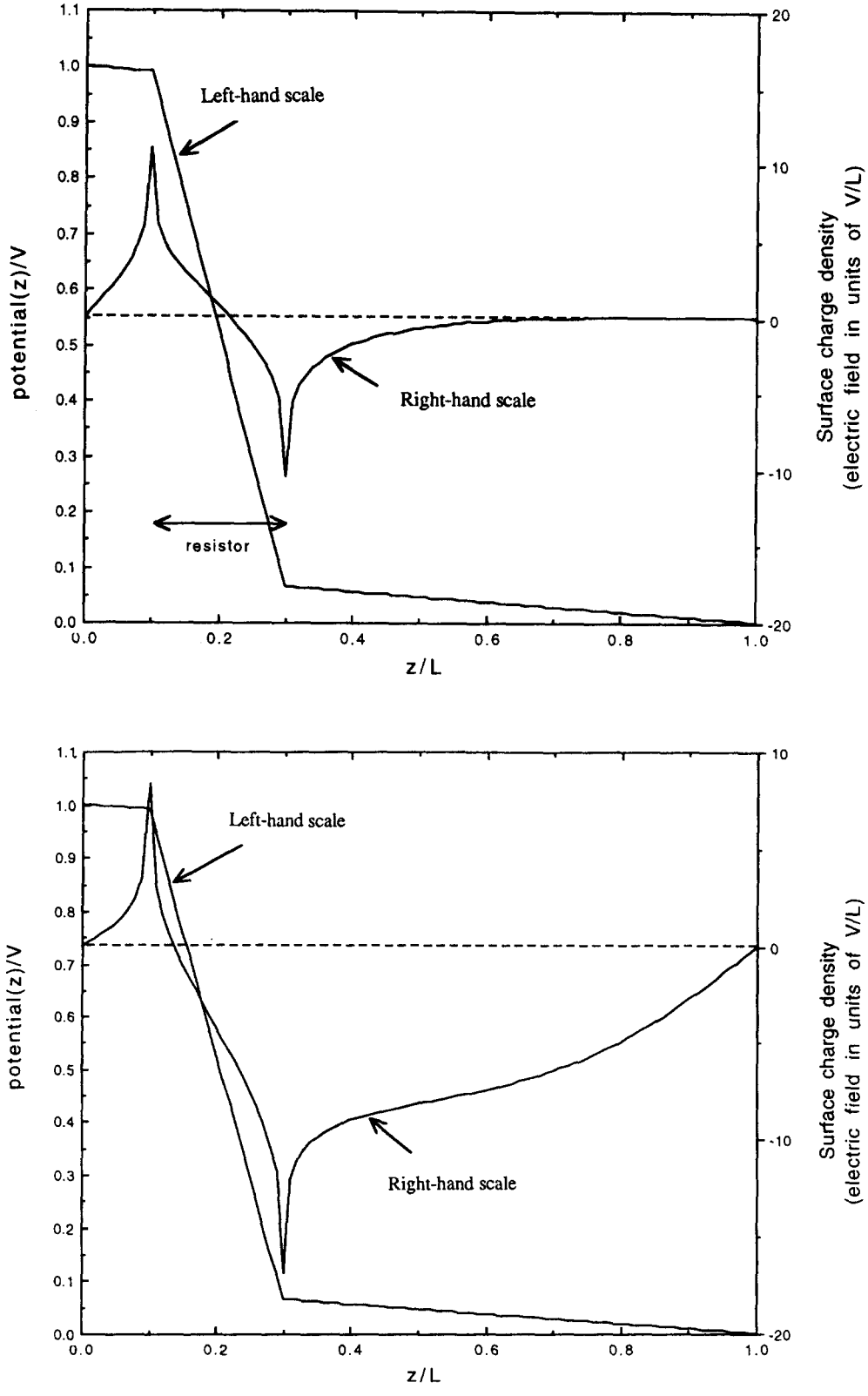

Fig. 3. Surface charge densities (radial electrical field at surface in units of V/L) and voltage drop (in units of V) along the wires and resistor for the off-set resistor and two locations of the battery of Fig. 2. When the voltage drop along the column is crudely the same as along the outer cylinder (Fig. 2, top), the surface charge density (top) is confined to the immediate neighborhood of the resistor. When the voltage distribution along the outer cylinder (Fig. 2, bottom) is very different from that along the column, the charge distribution along the wire (bottom) is large and negative for $z/L>0.3$ in order to produce the high radial electric field at the wire and maintain its potential near zero.

provide the electric field across the gap. When the circuit is closed by inserting the resistor, current flows and there are changes in the surface charges and the potential of various parts of the circuit, with the potential at any point around the circuit determined by current conservation and Ohm's law inside the wires and resistor, regardless of the circuit's geometrical configuration. But because the resistance of the rest of the circuit is small compared to that of the resistor, almost

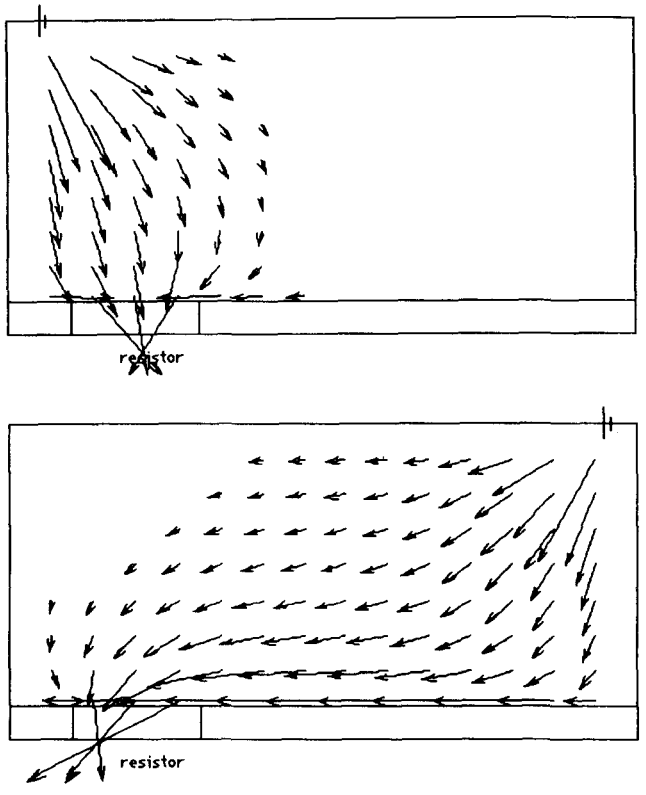

Fig. 4. Energy flow in the circuits of Figs. 2 and 3. The arrows represent relative values of the radial coordinate times the Poynting vector. The base of the arrow is at the point (ρ,z) where the Poynting vector is evaluated. At the surface of the column $(\rho=a)$, the points (ρ,z) are displaced upward slightly for clarity. Fluxes smaller in magnitude than the heads of the arrows are not shown.

all the potential drop occurs across the resistor, formerly the gap. The charge distribution and the electric field configuration at the resistor are changed in detail (there is now surface charge on the resistor itself, and at the internal interfaces between the wires and the ends of the resistor), but not as much as one might think. Away from the resistor terminals, the surface charges are much the same as in the absence of the resistor because the voltages around the circuit are largely the same. Depending on the configuration of the various parts of the circuit, the surface charge density on the wire near (but not at) the resistor may be of the same sign or opposite to that in the immediate neighborhood of the end of the resistor. Except in the most extreme situations, the surface charge distribution along the resistor itself is the intuitive one—positive at the end where the current enters and negative where it exits. What follows are explicit demonstrations of these remarks with the circuit of Fig. 1.

II. EXAMPLES OF SURFACE CHARGE DENSITIES ON THE WIRES AND RESISTOR AND ENERGY FLOW

The general features described in the introduction are now illustrated in the next several figures. Unless stated otherwise, the ratio of resistivities is $\rho_1/\rho_0=50$. Figure 2 presents the equipotentials for circuits with two different locations of the localized battery, while Fig. 3 shows the corresponding surface charge densities. Before noting the differences occasioned by the different positions of the battery, we comment on the grossest feature of the surface charge distributions. The charge is concentrated close to the ends of the resistor, with positive charge at the end where the current enters and negative charge where it leaves. Intuition would demand this behavior—there must be a strong electric field across the resistor to maintain the current flow in a medium of high resistivity. Care must be exercised with intuition, however, since the continuity of current flow and Ohm's law dictates that there is a discontinuity in the internal longitudinal electric field at the interface between wire and resistor. Thus there are internal surface charge densities at each end of the resistor. The charges on the free surface of the resistor do not necessarily relate to the current flow. In some situations, illustrated below, the sign of surface charge (and normal electric field) along the side of the wire seems to oppose the current flow, and in any event are unrelated to the small internal longitudinal electric field that drives the current in the highly conducting wire.

A. Influence of battery location

One influence of other parts of the circuit on the surface charge density is illustrated by comparison of the upper and lower surface charge densities in Fig. 3, corresponding to the two locations of the battery shown in Fig. 2. The resistor, of length $d/L=0.2$, is located near the bottom plate $(b/L=0.1)$. When the battery is near $z=0$ (Fig. 2, top), the potential drop is concentrated in the region of small z at all radial distances. Above the top of the resistor $(z/L>0.3)$, the potential within the column is less than 8% of its peak value, in rough correspondence with the other parts of the circuit. The surface charge density (Fig. 3, top) is localized to the resistor and the nearby portions of the wires and is nearly symmetric about the midpoint of the resistor. In contrast, when the battery is placed near the top of the cage (Fig. 2, bottom), the potential changes from being at its peak value for almost all z values at the cage $(\rho=R=0.5L)$ to being near zero on the top wire $(\rho\leq a,\ 0.3<z/L<1)$. Only a short distance away, the potential has appreciable positive values; the closeness of the contours implies a large radial electric field at the wire. In consequence, the surface charge density becomes skewed (Fig. 3, bottom), with an extensive negative surface charge density along most of the top wire.[34]

B. Energy flow from battery to resistor

The second role of the surface charge densities, the provision of the electric field throughout the space between the circuit elements, is important for the pattern of energy flow described by the Poynting vector, $\mathbf{S}\propto\mathbf{E}\times\mathbf{B}$. The magnetic field vanishes outside $(z<0,\ z>L,$ or $\rho>R)$, and in the interior region is purely azimuthal and given by Ampère's integral law, $B_\phi\propto\rho/a^2$ for $0<\rho<a$ and $B_\phi\propto 1/\rho$ for $a<\rho<R$. This (perhaps initially surprising) result follows from the observation that all the current flows (in the column, top and bottom plates, and outer cage) give rise to only azimuthal magnetic fields that are functions of ρ alone—just apply the right-hand rule! The remarks on p. 170 of Ref. 15 not withstanding, we may examine the contributions of the current flow in the different segments of the circuit. The flow in the z direction within the column and in the axially symmetric return path of the outer cage clearly lead to only an azimuthal component of $\mathbf{B}$ with no ϕ dependence. The surface current density on the top and bottom plates is radially outward and independent of azimuth, decreasing inversely with radius for $\rho>a$. Application of the right-hand rule to succes-

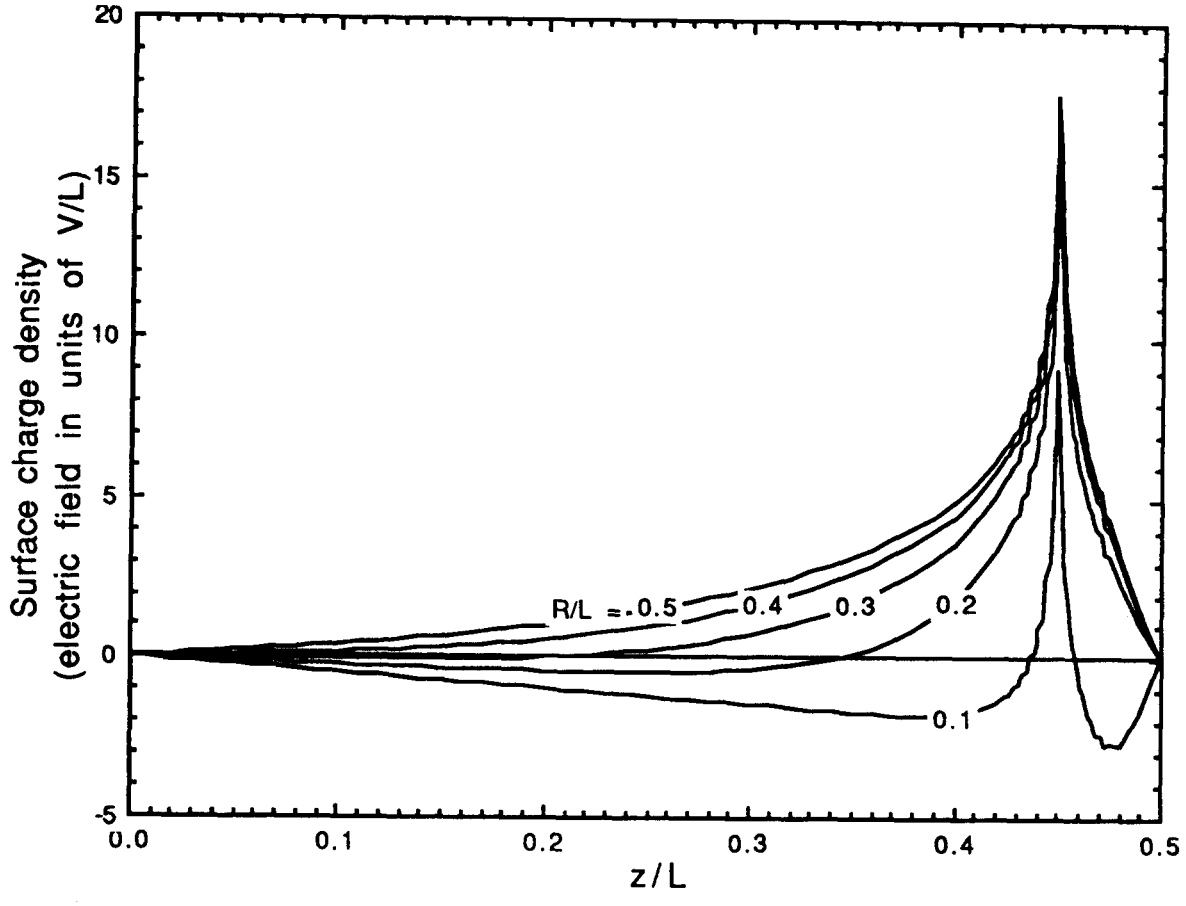

Fig. 5. Surface charge density (radial electric field at surface in units of V/L) on the bottom wire and bottom half of the resistor for different values of battery cage radius R. Battery and resistor are centered in z: column radius $a/L=0.05$, length of resistor $d/L=0.1$, length of wires $b/L=0.45$, battery thickness $d'/L=0$, battery location $b'/L=0.5$; resistivity ratio $r=50$. For the smallest R/L values, the proximity of the battery cage influences the surface charge distribution away from the end of the resistor, and even at its end.

sive infinitesimal pie-shaped segments of current flow on each plate shows that the sum of these contributions will result in only a ϕ component of **B**, with the discontinuity in B_ϕ decreasing as $1/\rho$ for $\rho>a$. Once the magnetic field is established to be azimuthal and independent of azimuth, it is safe to apply Ampère's integral law to a centered circular path of radius ρ at fixed z to determine its value (and dependence on z and ρ). For $\rho<R$ and $0<z<L$ we find the standard result, as if the wire were infinitely long. If either or both of ρ and z are outside those ranges, we find $\mathbf{B}=0$. In fact, apart from the central column not being a thin conducting tube, our circuit is an ideal toroid, with its well-known magnetic field.

The components of the Poynting vector are evidently only radial and axial: $S_\rho \propto -E_z B_\phi \propto -E_z/\rho$, $S_z \propto E_\rho B_\phi \propto E_\rho/\rho$. In Fig. 4 we display for the two battery positions of Fig. 2 the relative values of components of $2\pi\rho\mathbf{S}(\rho,z)$, the integral over azimuth of the Poynting vector, because that is the meaningful quantity in making a two-dimensional projection of the azimuthally symmetric three-dimensional circuit. The base of each vector is at the point (ρ,z) where **S** is evaluated, while its length is proportional to $2\pi\rho|\mathbf{S}|$. The flow of energy from the battery to the resistive components is evident. Its pattern in space is governed by the magnetic and electric fields there, the latter determined by the locations and sizes of the resistor and battery, as well as the resistivity ratio. Noteworthy is the significant axial flow of energy toward the resistor outside, but close to, the central column, especially visible in the bottom part of Fig. 4. This flow is proportional to E_ρ, that is, to the surface charge density. The choice of a much smaller value of resistivity ratio (e.g., $r=5$) is necessary to show clearly the small radially inward component of **S** at the surface of the wires (proportional to E_z), although it is very visible for the resistor.

Despite these diagrams there may be a lingering belief that much of the energy flows *within* the wires from battery to resistor. Quite the contrary! Within the central column there is an azimuthal magnetic field proportional to ρ and only an axial electric field, largest in the resistor. The Poynting vector points *radially inward* everywhere within the wires and resistor. It is proportional to ρ and corresponds to uniform energy deposition (heating) throughout a column segment of a given resistivity. Most of the heating is in the resistor, of course, as the lengths and directions of the arrows in Fig. 4 just outside the column indicate.

The reader may wish to ponder the reason for the similarities between Fig. 4 (Poynting vector) and Fig. 2 (potential), special to some particular geometries and current flows.[27]

C. Influence of proximity of other circuit elements

Figure 5 demonstrates another aspect of the influence of the rest of the circuit, the proximity of the cage to the column. This time the battery and resistor are both centered at $z/L=0.5$. The resistor is small and stubby ($d/L=0.1$, $a/L=0.05$). Only half of the range in z is shown. The other half

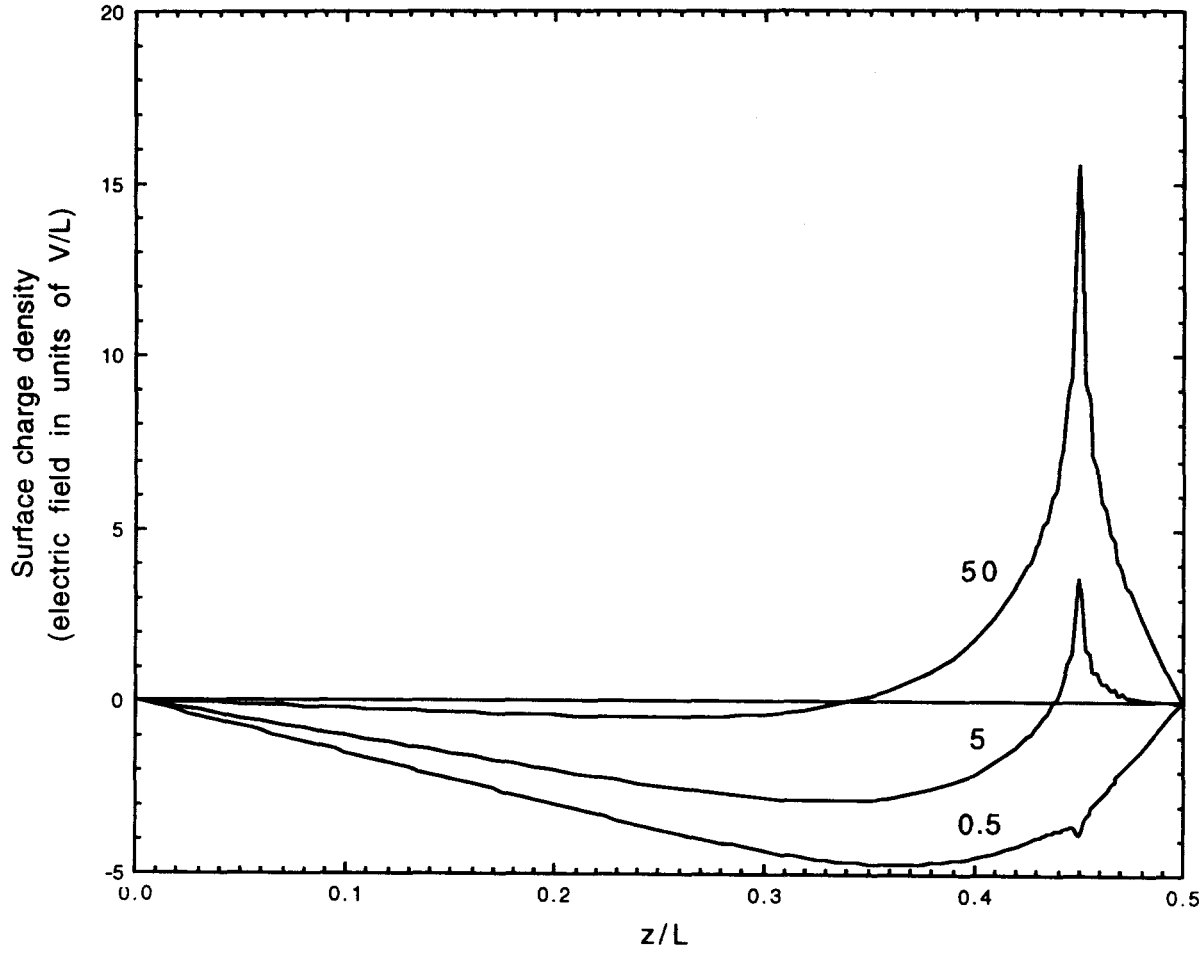

Fig. 6. Surface charge density (radial electric field at surface in units of V/L) versus z/L for three different resistivity ratios, $r=0.5$, 5, and 50, for a centered battery and resistor. Column and outer cylinder parameters are the same as in Fig. 5, with $R/L=0.2$. The $r=0.5$ example can be thought of two resistors (lead) with a wire (iron) between. The $r=5$ (50) example might be resistor/wires of tin/gold or iron/gold (steel/copper or nichrome/aluminum).

can be generated by reflection through the point ($x=0.5$, $y=0$). There is very little change in the surface charge density right at the end of the resistor (and not much change further away) for $R/L>0.4$. For smaller R values, the proximity of the cage and its particular variation of voltage with z begins to influence the surface charge. For $R/L=0.1$, the intuitive positive spike at the end of the resistor is still present, but otherwise the charge density is of opposite sign, even on most of the bottom half of the resistor. This counterintuitive behavior along the resistor can be traced to the circumstance that the potential on the nearby cage is a step function at $z/L=0.5$, while the potential drop across the resistor is linear from $z/L=0.45$ to $z/L=0.55$. The reader more comfortable with field lines is invited to draw sketches of those for large and small R/a ratios in order to understand the peculiarities of the surface charge density as a function of z.

D. Different conductivity ratios

Figure 6 illustrates the effect of different conductivity ratios (and so different voltage drops along the wires and resistor) on the surface charge distributions for a resistor and battery both centered in z. The parameters are the same as in Fig. 5, except that $R/L=0.2$ is fixed and the resistivity ratios are $r=0.5$, 5, and 50. The intuitive spike is smaller, the smaller the resistivity ratio, in accord with the smaller potential drop across the resistor ($\delta V/V\approx 0.85$ for $r=50$, $\delta V/V\approx 0.36$ for $r=5$). Away from the end of the resistor, the surface charge density is negative, the more so the smaller the resistivity ratio, because the potential along the bottom wire (determined by the resistive properties of the column) is decreasing in z more rapidly while the cage potential at the same z is still at its peak value. Larger radial electric fields occur for smaller resistivity ratios and are reflected in the surface charge density along the wire. The example of $r=0.5$ should be compared with those for $r>1$. It can be thought of as two symmetric resistors of length b (perhaps made of lead) separated by a (iron) wire of length d.

III. COMPARISON OF SURFACE CHARGE DISTRIBUTIONS FOR CLOSED AND OPEN CIRCUITS

We now turn to the comparison of the surface charge distributions for the closed circuit of Fig. 1 and the previous section with those of the electrostatic system of conductors (called open circuit, for brevity) obtained by removing the high resistivity segment of the central column (shaded part in Fig. 1). For simplicity and to have a finer mesh in the relaxation calculations, we consider only resistors and batteries

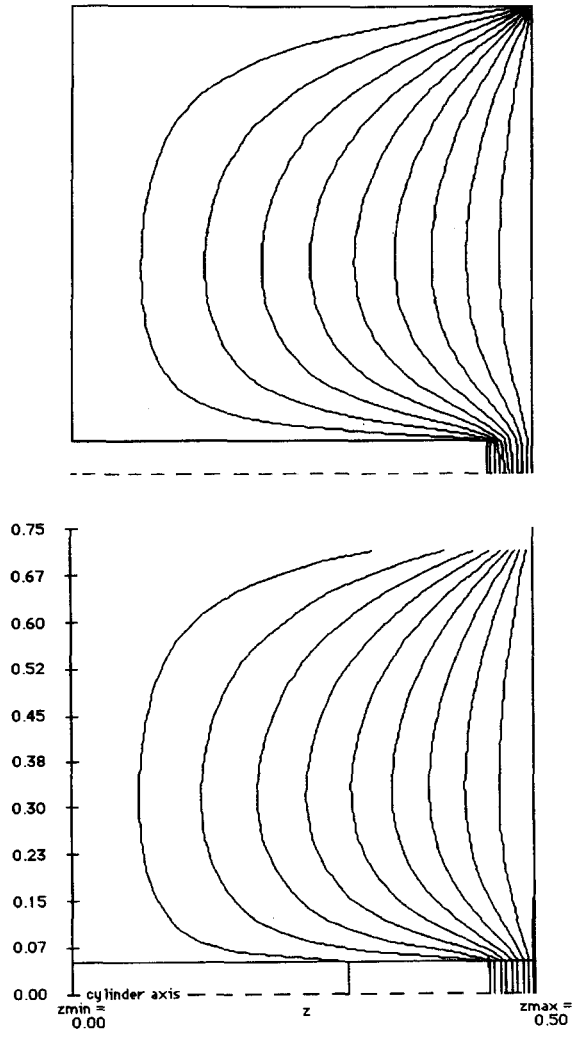

Fig. 7. Equipotential contours for the bottom half ($0 \leq z/L \leq 0.5$) of the open circuit (top) and closed circuit (bottom) for centered battery and resistor. Resistivity ratio $r=50$; column radius $a/L=0.05$ (4), outer cage radius $R/L=0.75$ (60), half-resistor length $d/2L=0.05$ (4), length of wires $b/L=0.45$ (36). Numbers in parentheses are the mesh units for the relaxation calculation of the open circuit. Potential contours (left to right) are $\Phi/V=0.95$ (0.05) 0.50.

that are centrally located in z. We can then use the lower half of the cylinders ($0 \leq z/L \leq 0.5$) and determine the behavior in the upper half by symmetry arguments.

A word needs to be said about the accuracy of the relaxation calculations in the cylindrical geometry. A coordinate transformation is needed to convert the azimuthally symmetric Laplace equation in ρ and z into an equation with a Cartesian Laplacian (See Appendix B). If the boundary of the two-dimensional region contains the z axis ($\rho=0$), special methods are needed to avoid serious loss of precision. Even if the z axis is excluded, errors creep in if the smallest value of ρ is only a few mesh points away from the axis. To establish plausible limits, sample relaxation calculations for the surface charge density were performed with the closed circuit and compared with the "analytic" Bessel–Fourier series solution of Appendix A. (An example is given in Fig. 10, for which the 40×60 lattice had a central column radius of 4, equivalent to column radius $a/L=0.05$. The agreement between the two calculations is very satisfactory, except for the one point exactly at the end of the resistor, where the finite mesh size causes a rounding off of the distribution. Smaller radii show some differences, but even at a radius of 2 units, the results are only slightly poorer than those shown in Fig. 10.)

The potential contours for the bottom half ($0 \leq z \leq 0.5$) of the circuit with a centered battery and centered resistor are shown in Fig. 7 for the open and closed circuits with a resistivity ratio of 50 for the latter. The potential patterns are nearly identical, with only a slight broadening toward $z=0$ for the closed circuit—the $\Phi=0.95$ V contour reaches the resistor at $z/L \approx 0.3$, not at $z/L>0.45$. With the potentials around the circuit in the two situations so similar, it is not surprising that the surface charge densities (on both the sides of the column and the ends of the wires) shown in Fig. 8 are so similar. In the open circuit, the flat termination of the end of the wire results in a singular charge density at the circular edge, varying as $\xi^{-1/3}$ where ξ is the limiting distance from the edge, either in z or in ρ.[35] The discrete mesh of the relaxation method cannot exhibit such a singularity, but it is integrable and so the total amount of charge can be estimated reliably. Note that, while the charge at the interface of the wire and resistor is less than the charge on the end of the wire with the resistor absent, there is charge on the side of the resistor ($z/L>0.45$), not present in the open circuit. It is as if the installation of the resistor causes mainly a rearrangement of the charge in the immediate neighborhood, without much change elsewhere—more on this subject in the next section.

The quantitative changes that occur with changes in the resistivity ratio are shown in Fig. 9. With a resistivity ratio $r=500$, the charge densities on the side of the wire are essentially identical, whether current is flowing or not. Even the end and interface densities approach each other, at least on axis. When $r=5$, the surface charge is much diminished for the closed circuit as compared to the open, but still peaks at the end of the resistor.

IV. COMPARISON OF TOTAL CHARGES ON CENTRAL COLUMN FOR OPEN AND CLOSED CIRCUITS

A final aspect is the total charge or capacitance associated with a resistor and its leads, compared with the charge or capacitance of the leads without the resistor. We consider the total charge on the bottom wire of our circuit (and the charge on the adjacent one half of the resistor, when present) for a symmetrically placed resistor and "battery" (either battery of zero thickness at $z/L=0.5$, or the linear voltage drop along the cage). The top wire (and half resistor) have equal and opposite charge. The charge on the flat top and bottom discs and on the cage at $\rho=R$ are not included. In the open-circuit calculations, the total charge on the wire is determined via Gauss's law, with a surface of integration removed from the conducting surfaces in order to assure an integrand that is as smooth as possible. For the closed circuit, the charge densities are integrated analytically before summation of the series.

Comparisons between the total charges on the half-column, with and without the resistor, are given in Tables I and II for various aspect ratios of the resistor for a resistivity ratio of 50. In Table I, the resistor is short, of length $d/L=0.1$, while the column radius is varied from $a/L=0.025$ to

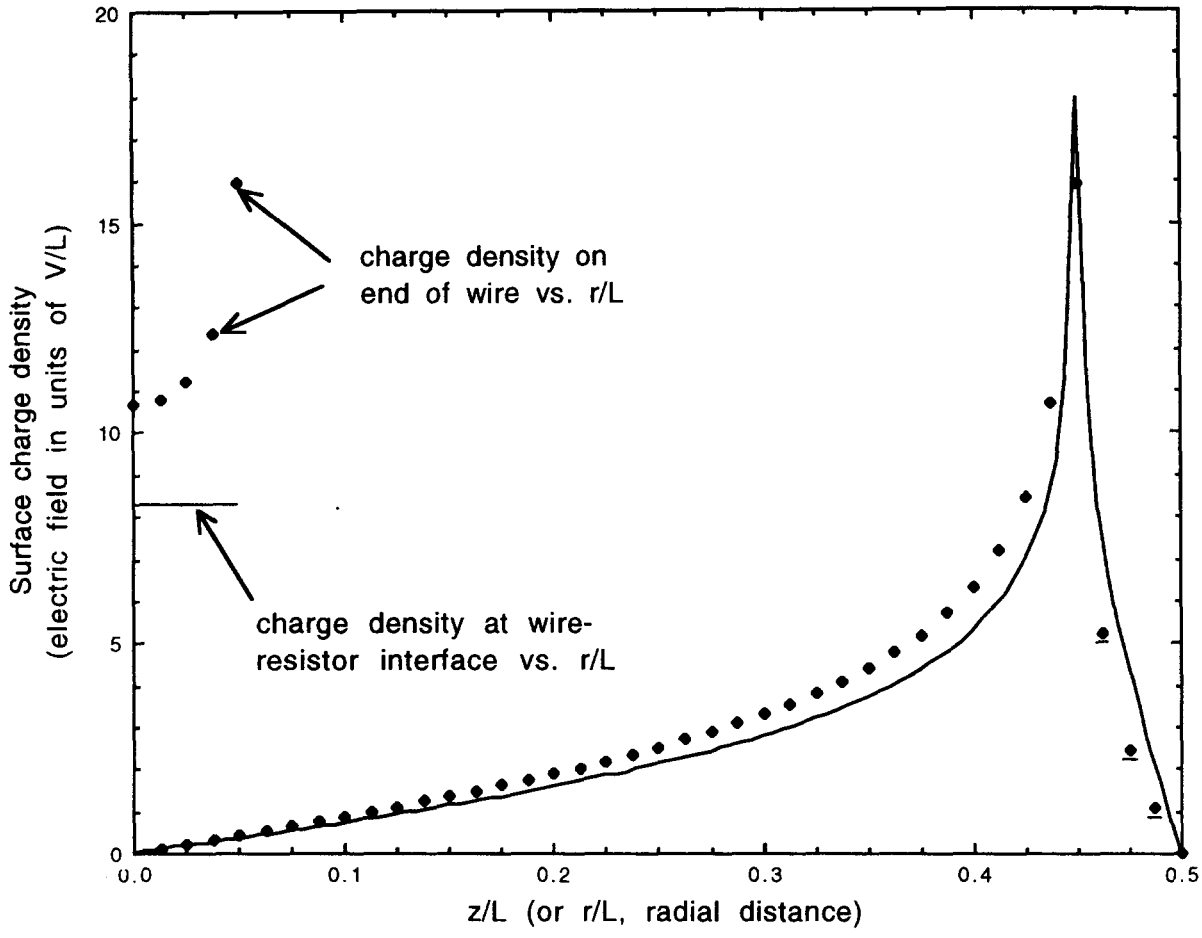

Fig. 8. Surface charge densities along the side and end of the bottom wire for the open circuit (solid points) and along the side and interface between wire and resistor for the closed circuit (continuous curves). The line and points at the left, extending in r/L to $a/L=0.05$, are for the interface and end. The configuration and parameters are the same as in Fig. 7, with resistivity ratio, $r=50$. The last three underlined points on the right are values of the radial electric field at $\rho=a$ in the gap beyond the end of the wire ($z/L>0.45$).

0.250. The resistor's aspect ratio thus varies from that of soup can to a deep-dish apple pie. In units of Va, the total charge in either situation varies by approximately 15%–20% as a function of a/L, except for the smallest a/L value. The ratio of the closed-circuit charge to the open-circuit charge varies by only 2%–3% as a/L changes by a factor of 10, and is $Q_{\text{closed}}/Q_{\text{open}}=0.85$–$0.88$ for both styles of battery. With a centered battery, but a resistivity ratio of 5, $Q_{\text{closed}}/Q_{\text{open}}=0.253\rightarrow0.263$ for the same range of a/L. For a resistivity ratio of 500, $Q_{\text{closed}}/Q_{\text{open}}=1.04\rightarrow1.01$ as $a/L=0.025\rightarrow0.250$. The approach of the ratio to unity as $r\rightarrow\infty$ is not universal, but a reflection of the large ratio of radius to gap. Only in the limit of $a/d\gg1$ (and $r\rightarrow\infty$) will both charges approach the naive parallel plate capacitor result with negligible fringing fields.

Results for the same resistivity ratio of 50, but a longer resistor ($d/L=0.4$) and a different set of aspect ratios, are presented in Table II (for a centered zero-thickness battery). For $a/L=0.025$, the two numbers for Q_{open} are for two different Gauss's law surfaces; for larger a/L, the two surfaces yielded the same results to within less than 0.3%. Here the different aspect ratio of the resistor leads to $Q_{\text{closed}}/Q_{\text{open}}$ larger than unity by 5%–20% for $r=50$.

Table III addresses the question of behavior of the ratio of charges as a function of resistivity ratio for the longer resistor of Table II. For each value of a/L there is a monotonic increase of the ratio with increasing r. The small differences between $r=500$ and $r=2000$ show that the limiting values for $r\rightarrow\infty$ cannot be much greater (independent investigation confirms this belief). The ratio does not approach unity, at least for the range of geometries shown. As indicated above, the differences in detail of the charge distributions for the closed and open circuits precludes a ratio of unity except in the extreme circumstances of the wires separated by a gap (resistor) that is very small compared to their diameter [for which almost all the charge is found on each end surface (interface)]. Even at the largest a/L value in Table III, the aspect ratio is only $2a/d=5/4$.

The sampling of results in Tables I–III indicates that, at least for practical resistors with large resistances compared to the connecting leads, the total charge or equivalently the capacitance of the resistor-leads combination is approximately the same (at the 15%–25% level) as is found for the same circuit configuration, but with the resistor removed. If one speaks of the capacitance of the wires for the open circuit, one may equally speak of the capacitance of the wires and resistor. A resistor and its leads are one extreme of a lossy capacitor, with rather less capacitance for its resistance than one expects from a useful capacitor.

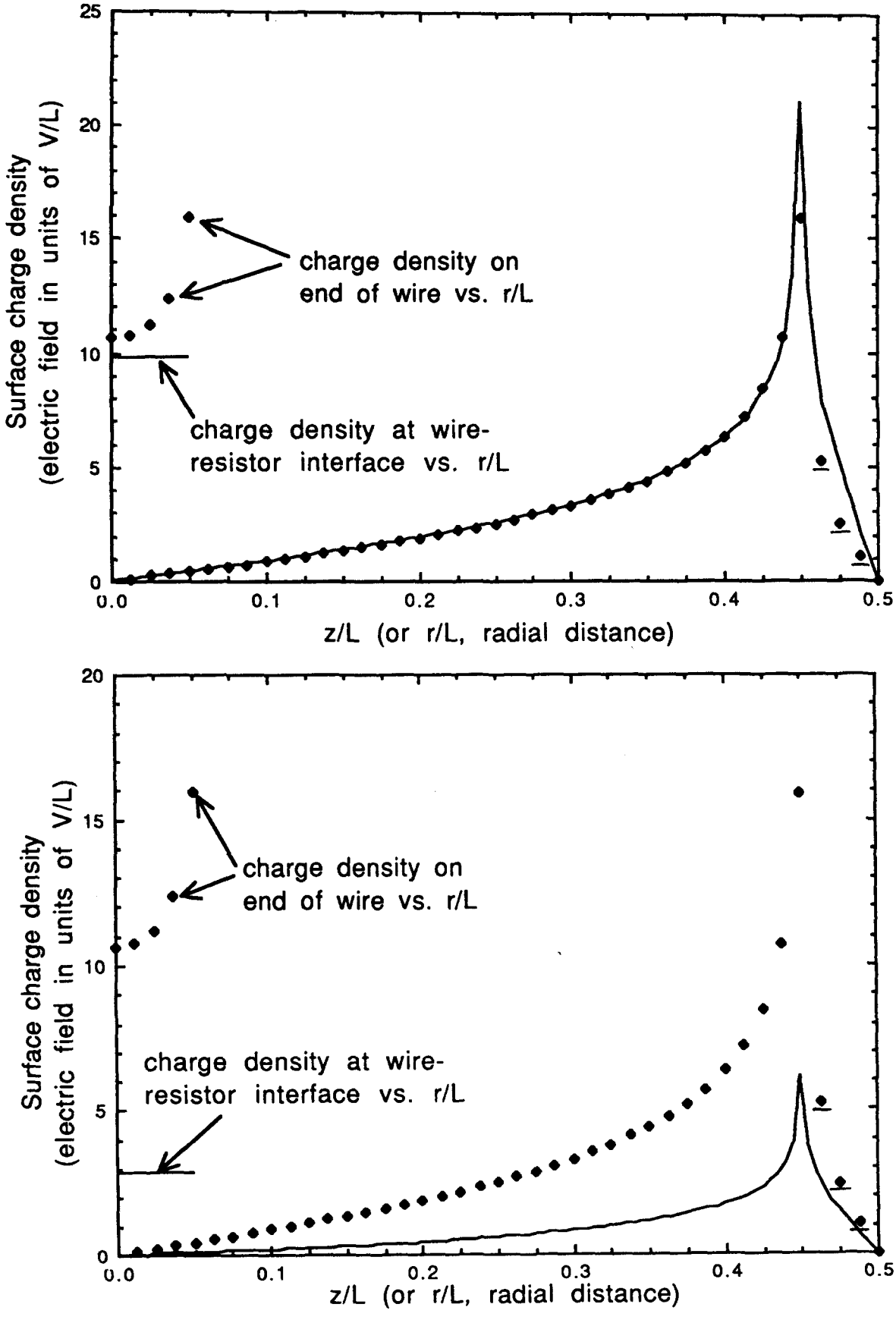

Fig. 9. The same as Fig. 8, except that the resistivity ratio between resistor and wire is $r=500$ (top) or 5 (bottom). The lines and points at the left, extending in r/L to $a/L=0.05$, are for the interface and end.

Table I. Charges on one wire (and one half of the resistor, for the closed circuit) for a symmetrically located gap or short resistor (length $d/L=0.1$) as a function of wire radius, a, for centered battery and linear potential drop at $\rho=R$. Resistivity ratio for the closed circuit, $r=50$, outer cylinder radius $R/L=0.75$. Charges in units of Va (equivalent to capacitances in units of a or $4\pi\epsilon_0 a$).

	Centered battery at $\rho=R$			
	Resistor absent	Resistor present		Ratio
a/L	Q_{open}	Q_{closed}	Q_{interf}/Q_{side}	Q_{closed}/Q_{open}
0.025	1.16	1.014	0.054	0.87
0.050	0.918	0.797	0.150	0.868
0.075	0.859	0.748	0.263	0.871
0.100	0.859	0.745	0.386	0.868
0.150	0.914	0.788	0.654	0.861
0.200	0.999	0.855	0.944	0.855
0.250	1.094	0.932	1.258	0.852
	Linear potential drop at $\rho=R$			
0.025	1.20	1.062	0.051	0.88
0.050	0.947	0.833	0.142	0.879
0.075	0.893	0.781	0.249	0.875
0.100	0.892	0.777	0.364	0.872
0.150	0.950	0.823	0.609	0.866
0.200	1.040	0.896	0.864	0.862
0.250	1.143	0.981	1.124	0.858

V. SUMMARY

We have explored the stationary surface charge densities in simple circuits with a special circuit of a battery, resistor, and connecting wires (Fig. 1) that possesses enough symmetry to be amenable to analytic solution but enough flexibility to illustrate how the surface charges on the resistor and nearby wires are influenced by other parts of the circuit. Surface charge densities play multiple roles—(1) they participate in providing the internal electric field that causes current to flow within the conducting elements of the circuit; (2) they participate in maintaining the potential around the circuit, especially on those elements obeying Ohm's law; (3) they establish the electric fields outside the circuit elements. The second role can cause counter-intuitive distributions of surface charge, as they provide along part of the circuit the voltage variation dictated by the current flow and Ohm's law, despite countervailing tendencies caused by other nearby parts of the circuit. To illustrate the third role, we show two examples of the pattern of flow of energy from battery to resistive components.

Table II. Charges on one wire (and one half of the resistor, for the closed circuit) for a symmetrically located gap or longer resistor (length $d/L=0.4$) as a function of wire radius, a, for centered battery at $\rho=R$. Resistivity ratio for the closed circuit, $r=50$, outer cylinder radius $R/L=0.75$. Charges in units of Va (equivalent to capacitances in units of a or $4\pi\epsilon_0 a$).

	Centered battery at $\rho=R$			
	Resistor absent	Resistor present		Ratio
a/L	Q_{open}	Q_{closed}	Q_{inter}/Q_{side}	Q_{closed}/Q_{open}
0.025	0.533/0.524	0.652	0.023	1.22/1.24
0.050	0.398	0.472	0.067	1.187
0.075	0.358	0.413	0.121	1.154
0.100	0.343	0.387	0.182	1.130
0.150	0.338	0.371	0.317	1.129
0.200	0.347	0.372	0.471	1.071
0.250	0.359	0.379	0.646	1.056

Table III. Ratio of closed to open circuit charges on one wire (and one half of the resistor, for the closed circuit) for a symmetrically located gap or resistor and battery, as in Table II, but for four different resistivity ratios, $r=5$, 50, 500, 2000.

a/L	$r=5$ Q_{closed}/Q_{open}	$r=50$ Q_{closed}/Q_{open}	$r=500$ Q_{closed}/Q_{open}	$r=2000$ Q_{closed}/Q_{open}
0.025	0.757/0.771	1.22/1.24	1.28/1.30	1.29/1.31
0.050	0.735	1.187	1.244	1.249
0.075	0.714	1.154	1.210	1.215
0.100	0.697	1.130	1.186	1.191
0.150	0.672	1.129	1.151	1.155
0.200	0.651	1.071	1.125	1.130
0.250	0.634	1.056	1.110	1.115

For resistors with a resistance large compared to that of the connecting wires and other components, the potential variation around the circuit with current flowing is quite similar to that when the resistor is removed—almost all the voltage drop occurs across the resistor. We are thus led to an instructive comparison of the surface charge distributions for closed and open circuits (resistor present vs. resistor removed), the latter computed by a relaxation technique. While differing in detail in the immediate neighborhood of the resistor or gap, the charge distributions are surprisingly similar. The ratio of total charge on the lead wires and resistor to that of the wires alone (for the open circuit) is not far from unity for large resistivity ratios—the resistor and leads, a lossy capacitor, has a "capacitance" that can be estimated from the open circuit of leads without the resistor.

Two appendices contain the mathematical and computational details.

ACKNOWLEDGMENTS

I thank Susan Lea and John Burke of San Francisco State University for bringing this problem to my attention and the referee for helpful comments. I thank Wayne Saslow of Texas A&M University for valuable discussions on both the physics and its presentation.

APPENDIX A: ANALYTIC BESSEL–TRIGONOMETRIC SERIES SOLUTION FOR THE CLOSED CIRCUIT WITH RESISTOR

The circuit shown in Fig. 1 consists of a central right-circular conducting cylinder of radius a and length L with three segments—two ($0<z<$b and $b+d<z<L$) with resistivity ρ_0 and one ($b<z<b+d$) with resistivity ρ_1. At $z=0$ and $z=L$ are fastened two circular plates of radius R, assumed of zero resistivity (and so equipotentials, even with current flowing). At radius R is a cylindrical cage such that the potential on that surface is

$$\Phi(R,z)=\begin{Bmatrix} V \\ V(b'+d'-z)/d' \\ 0 \end{Bmatrix} \quad \text{for} \quad \begin{Bmatrix} 0<z<b' \\ b'<z<b'+d' \\ b'+d'<z<L \end{Bmatrix}. \tag{A1}$$

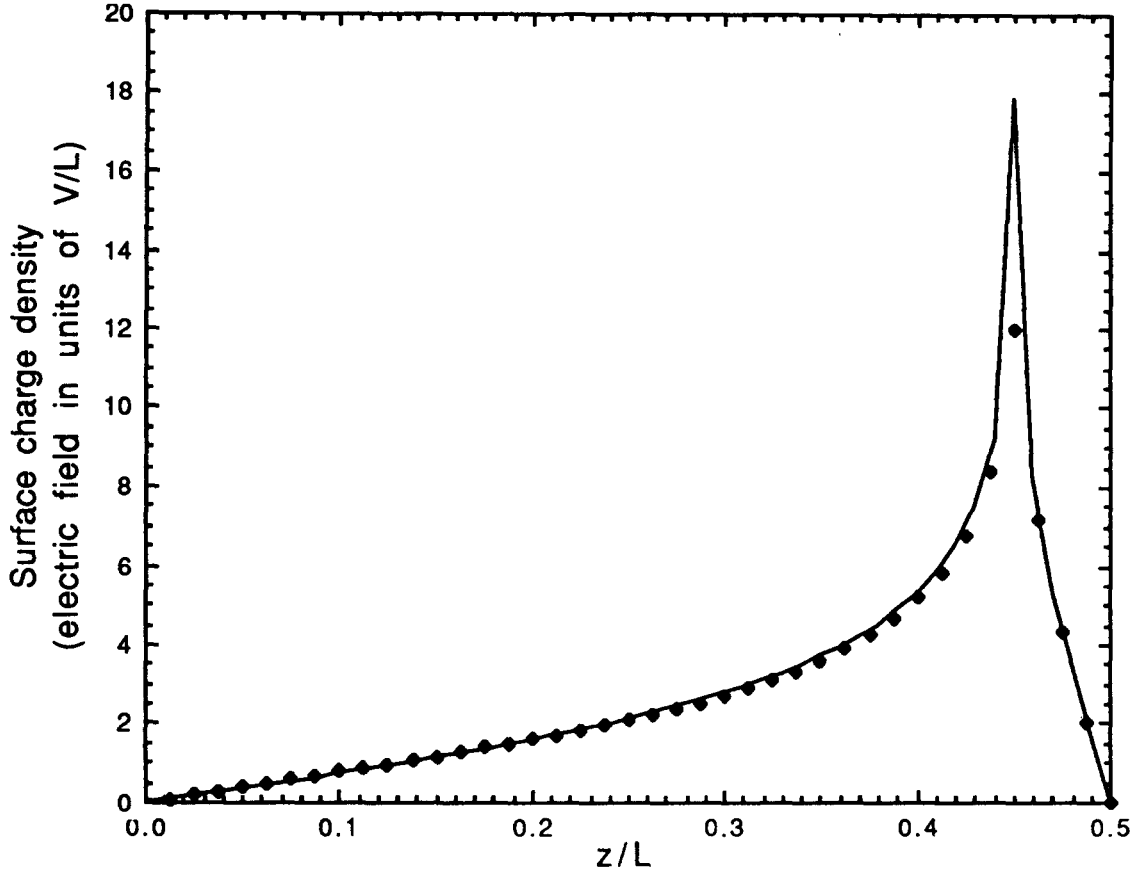

Fig. 10. Comparison of the wires-resistor surface charge density calculated via the relaxation method (solid points) with the results of the analytic Bessel–Fourier series solution (continuous curve) for a resistor (length $d/L=0.1$) and battery centered in z ($d'=0$, $b'/L=0.5$). Other parameters: resistivity ratio $r=50$; outer cage radius $R/L=0.75$, column radius $a/L=0.05$, wires length $b/L=0.45$. The relaxation grid is 40×60 with column radius of 4 units.

In the limit $d'\to 0$, the potential is a "ring" battery with a sudden drop in potential at $z=b'$. For $b'=0$, $d'=L$, there is a uniform potential drop along the surface, $\Phi(R,z)=V(1-z/L)$. Such a cage is a type of distributed battery. Such cages exist, at least in approximate form—the outer set of electrodes of a time-projection chamber (TPC) is one example.[33]

The potential inside and on the surface of the central cylinder (the slightly lossy wires and resistor of the circuit) can be found by elementary means. Explicitly, we have, for $0<\rho\leqslant a$,

$$\Phi_{\text{inside}}(z)=\Phi_{\text{surface}}(z)=\left\{\begin{array}{c} V-\alpha z \\ \beta-r\alpha z \\ \alpha(L-z)\end{array}\right\}\quad\begin{array}{l}(0<z<b)\\(b<z<b+d),\\(b+d<z<L)\end{array} \tag{A2}$$

where $r=\rho_1/\rho_0$ is the ratio of resistivities and

$$\alpha=\frac{V}{[L+(r-1)d]};\quad \beta=\frac{[L+(r-1)(b+d)]}{[L+(r-1)d]}\cdot V. \tag{A3}$$

The electric field in the wire segments is $E_z=\alpha$; in the resistor it is $E_z=r\alpha$.

Because the tangential component of electric field is continuous in passing from inside the resistive column ($\rho<a$) to the space beyond ($a<\rho$), the potential just outside the resistive column is given by (A2). The solution to the Laplace equation in the space bounded by the two cylinders and end plates, with the potential now specified on all the interior surfaces, can be found by use of the appropriate azimuthally symmetric Dirichlet Green function:[36]

$$\begin{aligned}G_D(\rho,z;\rho',z')=\frac{4}{L}\sum_1^\infty\ &\sin(n\pi z/L)\\ &\times\sin(n\pi z'/L)\frac{1}{f_n}\,[I_0(n\pi\rho_</L)\\ &-I_0(n\pi a/L)K_0(n\pi\rho_</L)/K_0(n\pi a/L)]\\ &\times[K_0(n\pi\rho_>/L)\\ &-K_0(n\pi R/L)I_0(n\pi\rho_>/L)/I_0(n\pi R/L)]\end{aligned} \tag{A4}$$

where

$$f_n=1-\frac{K_0(n\pi R/L)I_0(n\pi a/L)}{K_0(n\pi a/L)I_0(n\pi R/L)}. \tag{A5}$$

The solution,

$$\Phi(\rho,z)=-\frac{1}{4\pi}\oint\Phi(\rho',z')\,\frac{\partial G_D}{\partial n'}\,da', \tag{A6}$$

requires the radial derivatives of G_D at $\rho=a$ and $\rho=R$:

$$\left(\frac{\partial G_D}{\partial \rho'}\right)_{\rho'=a} = \frac{4}{aL}\sum_1^\infty \frac{\sin(n\pi z/L)\sin(n\pi z'/L)}{f_n K_0(n\pi a/L) I_0(n\pi R/L)} [I_0(n\pi R/L)K_0(n\pi\rho/L) - K_0(n\pi R/L)I_0(n\pi\rho/L)], \tag{A7}$$

$$\left(\frac{\partial G_D}{\partial \rho'}\right)_{\rho'=R} = \frac{-4}{RL}\sum_1^\infty \frac{\sin(n\pi z/L)\sin(n\pi z'/L)}{f_n K_0(n\pi a/L) I_0(n\pi R/L)} [I_0(n\pi\rho/L)K_0(n\pi a/L) - K_0(n\pi\rho/L)I_0(n\pi a/L)]. \tag{A8}$$

To avoid the necessity of integrating over the end caps, we add to and subtract from the potential the term, $V(1-z/L)$, which satisfies the boundary conditions at $z=0$ and $z=L$. Straightforward calculation with (A6), (A7), and (A8) yields the solution

$$\Phi(\rho,z) = V(1-z/L) + \sum_1^\infty \frac{\sin(n\pi z/L)}{f_n} F_n(\rho,a,R), \tag{A9}$$

where

$$F_n(\rho,a,R) = B_n\left[\frac{K_0(n\pi\rho/L)}{K_0(n\pi a/L)} - \frac{K_0(n\pi R/L)I_0(n\pi\rho/L)}{K_0(n\pi a/L)I_0(n\pi R/L)}\right] + C_n\left[\frac{I_0(n\pi\rho/L)}{I_0(n\pi R/L)} - \frac{K_0(n\pi\rho/L)I_0(n\pi a/L)}{K_0(n\pi a/L)I_0(n\pi R/L)}\right] \tag{A10}$$

and the Fourier series coefficients are

$$B_n = \frac{2}{L}\int_0^L [\Phi_{\text{surface}}(z') - V(1-z'/L)]\sin(n\pi z'/L)dz' \tag{A11}$$

and

$$C_n = \frac{2}{L}\int_0^L [\Phi(R,z') - V(1-z'/L)]\sin(n\pi z'/L)dz'. \tag{A12}$$

With the potentials defined in Eqs. (A1) and (A2), the explicit forms of the Fourier coefficients are

$$B_n = \frac{2\alpha L(r-1)}{n^2\pi^2}\cdot[\sin(n\pi b/L) - \sin(n\pi(b+d)/L)],$$

$$C_n = \frac{2VL}{d'n^2\pi^2}[\sin(n\pi b'/L) - \sin(n\pi(b'+d')/L)]. \tag{A13}$$

The surface charge density[37] on the sides of the composite cylinder ($\rho=a$), $\sigma_s(z)=E_\rho/4\pi$, is

$$\sigma_s(z) = \frac{1}{4L}\sum_{n=1}^\infty \frac{n}{f_n}\left\{\begin{array}{l} B_n\left[\dfrac{K_1(n\pi a/L)}{K_0(n\pi a/L)} + \dfrac{K_0(n\pi R/L)I_1(n\pi a/L)}{K_0(n\pi a/L)I_0(n\pi R/L)}\right] \\ -C_n\left[\dfrac{I_1(n\pi a/L)}{I_0(n\pi R/L)} + \dfrac{K_1(n\pi a/L)I_0(n\pi a/L)}{K_0(n\pi a/L)I_0(n\pi R/L)}\right]\end{array}\right\}\sin(n\pi z/L). \tag{A14}$$

The charge density on the bottom plate is

$$\sigma_b(\rho) = \frac{V}{4\pi L} - \frac{1}{4L}\sum_1^\infty \frac{n}{f_n}F_n(\rho,a,R). \tag{A15}$$

The charge density at $z=b$, $0<\rho<a$, the interface between the resistor and the wire, is

$$\sigma_i(\rho) = (r-1)\alpha/4\pi, \quad 0<\rho<a. \tag{A16}$$

Of most interest is the charge distribution along the wire and the resistor, particularly in comparison with the corresponding distribution when the resistor is removed so that no current flows. The total charges on the various parts of the circuit can be found by straightforward integration. The expressions are not illuminating. We leave their calculation as an exercise for the enterprising reader. The sum of these charges Q_s, Q_b, and Q_i, divided by V can be interpreted as the capacitance of the whole resistor circuit. The sum, $(Q_s+Q_i)/V$, may be interpreted as the capacitance of the wire and resistor combined. For $a \ll R$, this capacitance is small compared to that of a circular disc capacitor consisting of the top and bottom plates. Nevertheless, it will be of interest in comparison with the corresponding capacitance of the electrostatic configuration of the same dimensions (and battery), but with the resistor absent.

In principle, the numerical computation is straightforward; in practice, some care needs to be taken. The Bessel functions $I_m(z)(K_m(z))$ grow (decrease) exponentially with z. It is prudent to examine the terms in the series of (A10) and (A14) for large n to isolate the large n behavior and make appropriate modifications in the details of summing the series. In the limit of ρ finite and $R\to\infty$, the solution simplifies: $f_n\to 1$, the terms in (A10) and (A14) multiplying C_n go to zero, and the second terms in the square brackets multiplied by B_n vanish. In exhibiting the results it is convenient to use ratios $(a/L, b/L, d/L, R/L)$ for the circuit dimensions and to express the potential in units of V and the surface charge density[37] in units of $V/4\pi L$ (the same numerically as the radial electric field in units of V/L) as functions of ρ/L and z/L. The necessary program was written using Symantec's Think Pascal software and run on a Macintosh LCII and (much faster) on a Macintosh Centris 650.

To obtain the potential for the original example[19–21] of an infinitely long resistive cylindrical wire of radius a, with internal electric field E_0, surrounded by a grounded cylinder of radius R, from Eq. (A9), we put $V=E_0L$, $z=z'+L/2$, and

$\Phi=\Phi'+V/2$. With $r=1$, $B_n=0$. We must average the potential for $d'=0$, $b'=0$ (battery at $z=0$) and $d'=0$, $b'=L$ (battery at $z=L$) to make $\Phi'=0$ at $\rho=R$. For $L\to\infty$, with fixed n and ρ, F_n/f_n has a well-defined limit. The resulting Fourier series in (A9) can be summed[38] to give

$$\Phi'(\rho,z)=-E_0 z'\,\frac{\ln(\rho/R)}{\ln(a/R)},\quad a\leqslant\rho\leqslant R. \tag{A17}$$

APPENDIX B: RELAXATION CALCULATION OF CYLINDRICAL OPEN AND CLOSED CIRCUITS WITH AZIMUTHAL SYMMETRY

The open circuit consists of an outer right-circular cylinder of radius R and length L having the potential given by Eq. (A1) on its surface, two circular conducting plates at each end, one at potential $V(z=0)$ and the other at zero potential $(z=L)$ and two solid, right-circular, conducting cylinders, one of length b and the other of length $(L-b-d)$, mounted on axis, in from each end. These cylinders, the wires of the circuit, have a gap between them of length $d=L-2b$ (the length of the resistor in the closed circuit). In contrast to the same geometry, but with the central region filled in by the resistor, the solution for the potential everywhere is not expressible in terms of an expansion in terms of known orthogonal functions. We resort to the numerical method of relaxation. The azimuthally symmetric cylindrical geometry poses some problems, happily surmountable, beyond the standard two-dimensional relaxation computations.

For convenience, the coordinates (ρ,z) are replaced by (y,x), respectively. The Laplace equation in cylindrical coordinates is, in terms of x and y,

$$\frac{\partial^2\Phi}{\partial x^2}+\frac{1}{y}\frac{\partial}{\partial y}\left(y\,\frac{\partial\Phi}{\partial y}\right)=0. \tag{B1}$$

With the substitution, $U(x,y)=\sqrt{y}\Phi(x,y)$, Laplace's equation for Φ is converted into a Poisson-like equation for U with a Laplacian in Cartesian coordinates:

$$\frac{\partial^2 U}{\partial x^2}+\frac{\partial^2 U}{\partial y^2}=-\frac{1}{4y^2}\,U. \tag{B2}$$

We apply the relaxation method to a square lattice with spacing h, labeling the lattice site at $x(i)=ih$, $y(j)=jh$ by the pair of integers (i,j). If $F(x,y)$ is a well-behaved function in the neighborhood of (i,j), but not necessarily harmonic, by explicit Taylor series expansions the "cross" sum,

$$S_1=F(i+1,j)+F(i,j+1)+F(i-1,j)+F(i,j-1), \tag{B3}$$

can be expressed as

$$S_1=4F(i,j)+h^2\nabla^2F+h^4(F_{xxxx}+F_{yyyy})/12+O(h^6), \tag{B4}$$

where the subscripts indicate partial differentiation and all quantities are evaluated at (i,j). Similarly, the "square" sum,

$$S_2=F(i+1,j+1)+F(i-1,j+1)+F(i-1,j-1)+F(i+1,j-1) \tag{B5}$$

can be expressed as

$$S_2=4F(i,j)+2h^2\nabla^2F-h^4(F_{xxxx}+F_{yyyy})/3+h^4\nabla^2(\nabla^2F)/2+O(h^6). \tag{B6}$$

If $\nabla^2F=0$ as in the conventional two-dimensional calculations, the averages $S_1/4$ and $S_2/4$ each give the value of $F(i,j)$, correct to order h^3 inclusive. An improvement can be obtained by forming the average,

$$\tilde{S}=\tfrac{1}{5}[S_1+\tfrac{1}{4}S_2]. \tag{B7}$$

The result is

$$\tilde{S}=F(i,j)+\frac{3}{10}\,h^2\nabla^2F+\frac{h^4}{40}\,\nabla^2(\nabla^2F)+O(h^6). \tag{B8}$$

If $\nabla^2F=0$, then $\tilde{S}$ gives $F(i,j)$, correct to order h^5 inclusive, and so gives higher accuracy than either S_1 or S_2 at the expense of doubling the number of computations per iteration. When $\nabla^2F\neq0$, (B8) has the advantage of permitting substitution of ∇^2F on the right-hand side for the solution of Poisson-like equations.

In our situation, where $\nabla^2U=-U/4y^2$, a lowest order approximation of the Laplacian of $U/4y^2$ [for the third term on the right of (B8)] leads to the iteration scheme,

$$U_{\text{new}}(i,j)=\tilde{S}(U_{\text{old}})+\frac{1}{20j^2}\,U_{\text{old}}(i,j)+\frac{1}{160j^2}\,S_1(U_{\text{old}}) \tag{B9}$$

or alternatively,

$$U_{\text{new}}(i,j)=\left[\tilde{S}(U_{\text{old}})+\frac{1}{160j^2}\,S_1(U_{\text{old}})\right](1-1/20j^2)^{-1}. \tag{B10}$$

We use (B10) in our computations, but (B9) works just as well.

It is obvious that there are likely to be difficulties at small j values (small radii). If the region of interest includes the axis there are potentially large errors. There are no infinities because the line segment at $y=0$ $(j=0)$ is specified to have $U=0$ along it, whatever the potential there (recall that $U=\sqrt{y}\Phi$). Nonetheless, if the axis is part of the three-dimensional region where the potential is desired, as it is in our situation, the axis is not a boundary "surface" and the potential is not given a priori there. Relaxation in U with $U=0$ on axis (and U having nonzero values on other surfaces) leads to a valid relaxation solution for U, but the values of the potential Φ on axis must be found by extrapolation from sites with $j\neq0$. Such a procedure is highly inaccurate in general, in part because all values of U on nearby boundary surfaces are scaled with $\sqrt{y}$ factors and so are small, whatever the potential on those surfaces.

For our geometry the problems associated with $y=0$ can be circumvented by using an approximate analytic solution of the Laplace equation in terms of a Bessel–Fourier series in the cylindrical region, $(0<\rho<a),(b<z<b+d)$. The boundary values of the potential are $\Phi=V$ at one end face and $\Phi=0$ on the other, while on the cylindrical surface $\rho=a$, Φ is known (to some accuracy) at a discrete set of points in z. If the potential were given as a function $\Phi(a,z)$ at every point along the cylinder, the problem would be exactly solvable in series form by quadrature. Given only n values Φ_k $(k=1,2,\ldots,n)$, an approximate solution can be found with a finite series of $O(n)$ terms. Suppose the Φ_k are the values of $\Phi=U/\sqrt{y}$ at the lattice sites (k,j_a) corresponding to $y=a$ and some set of i values. Then the approximate solution with those Φ_k can be used to calculate $U(k,j_a-1)$ for use in S_1

and S_2 to find new values of $U(k,j_a)$. After another iteration there is a new set of Φ_k; a new approximate solution can be found and a new set of $U(k,j_a-1)$.

The procedure is thus to set the region for relaxation as that bounded in x by $x=0$ and $x=L$, and in y by $y=a$ and $y=R$, with the potential fixed on the surfaces of the plates, $x=0$, $x=L$, the cage, $y=R$, and the wires, ($y=a$, $0<x<b$) and ($y=a$, $b+d<x<L$). The "gap" (former surface of the resistor), $y=a$, $b<h(b+d)$, is treated as part of the interior. At the start, a guess is made for $U(i,j)$ at all interior points. The "gap" values of U with $y=a$ and $b<x<b+d$ yield the Φ_k for the approximate analytic solution for $y<a$ and so the values of $U(k,j_a-1)$, which can be viewed as temporary true "boundary" values, to be used with the others in finding new values by iteration. After each iteration, the process is repeated. Since the approximate solution consists of a finite series of a few terms, the time spent in this subsidiary computation for each iteration is not excessive.

To find an approximate analytic solution in the region, $0<y<a$, $b<x<b+d$, with $\Phi=V_1$ at $x=b$ and $\Phi=V_2$ at $x=b+d$, we begin with the axially symmetric solution of the Laplace equation, assuming that the boundary value $\Phi(x,a)$ is a continuous known function,

$$\Phi(x,y)=\sum_{m=1}^{\infty} A_m I_0(m\pi y/d)\sin(m\pi x/d) + (V_2-V_1)x/d+V_1, \tag{B11}$$

where $I_0(z)$ is the modified Bessel function of the first kind of order zero; we have shifted the origin in x to $x=b$. The coefficient A_m is given by

$$I_0(m\pi a/d)A_m=\frac{2}{d}\int_0^d [\Phi(x',a)-(V_2-V_1)x'/d-V_1] \times\sin(m\pi x'/d)dx'. \tag{B12}$$

If $d=Nh$ and the function $\Phi(x,a)$ is replaced by a discrete set of evenly spaced values Φ_k at $x=kh$ ($k=1,2,3,\ldots,N-1$), we approximate the series of (B11) by the first $(N-1)$ terms, then put $x=kh$, $y=a$ for each k value in turn to obtain $(N-1)$ simultaneous linear equations for the $(N-1)$ coefficients A_m. The system can be inverted to find all $(N-1)A_m$. An equivalent and simpler alternative procedure is to limit the series in (B11) to the first $(N-1)$ terms and determine the coefficients A_m by approximating the integral in (B12) by a simple sum (trapezoidal rule),

$$I_0(m\pi a/d)A_m\approx\frac{2h}{d}\sum_{k=1}^{N-1} [\Phi_k-(V_2-V_1)kh/d-V_1] \times\sin(m\pi kh/d). \tag{B13}$$

Given a set of $U(i,j_a)$ values, we construct the Φ_k, compute the coefficients with (B13), then insert them into the finite series (B11) with $y=a-h$ ($j=j_a-1$) to find $\Phi(x(i),y=(j-1)h)$ and so $U(i,j_a-1)$. The relaxation iteration then proceeds according to (B10) for all the interior points of the lattice. When the iterations attain the desired degree of precision, the final $U(i,j_a)$ values are used to construct the potential (B11) for the region ($b<x<b+d$,$0<y<a$).

The relaxation technique can be applied in a straightforward way to the segmented resistive column, where the wires and "gap" now have known potentials from Eq. (A2). By comparison with the results of the analytic Bessel-trigonometric series we can assess the dangers of small inner radii. The region of interest is bounded in x by the planes $x=0$ and $x=L$ and in radius by the cylinders $y=a$ and $y=R$. The planes (circular discs) have zero resistivity; the plane $x=0$ has $\Phi=V$ and the plane $x=L$ has $\Phi=0$. The outer and inner cylinders now have potentials specified by (A1) and (A2). The relaxation computation is standard, with the potential known and fixed on all the boundaries. The only potential concern is the presence of the factors of $1/j^2$ in (B10). An example of the comparison of results for the surface charge density from the two methods is shown in Fig. 10 for $a/L=0.05$, $b/L=0.45$, $d/L=0.1$, $r/L=0.75$ and a resistivity ratio of 50. The relaxation computation has a lattice of 40×60 for the half-region, $0<x<L/2$. The inner cylinder has $j_a=4$. The comparison shows that, apart from the immediate neighborhood of the interface between the wire and the resistor, the radial derivatives of the potential agree quite well, even though in the relaxation computation the derivative is approximated at (i,j_a) by

$$hE_\rho=-h\partial\Phi/\partial\rho\approx 1.5\Phi(i,j_a)-2.0\Phi(i,j_a+1) +0.5\Phi(i,j_a+2). \tag{B14}$$

The lack of precise agreement at $x=b$ is expected since the axial derivative of the potential changes discontinuously there and the spacing between lattice sites is such that only three or four points lie in the peak region. The analytic and relaxation values of the potential in the interior agree very well.

The general agreement shown in Fig. 10 demonstrates that the relaxation technique works adequately for azimuthally symmetric potential problems down to quite small radii. For the open circuit problem, the approximate analytic series in the region near and at $\rho=0$ assures that the small radius "disease" can be circumvented. Only at sharp corners, where the charge densities are singular, does the discreteness of the lattice cause the relaxation technique to fail quantitatively.

For the open circuit, electrostatic situation, the capacitance of parts or all of the circuit can be determined through the use of Gauss's law to find the appropriate total charge. A path can be chosen away from the surfaces [e.g., in y for fixed $x=(b+L/2)/2$, or in x for fixed $y=a+2h$], so that the x or y derivative of the potential can be reliably estimated by a formula analogous to (B14), but symmetric, rather than one-sided. The sum of those derivatives weighted with $2\pi h^2 j$, is the trapezoidal estimate of the integral of the normal component of the electric field over the surface. Simpson's rule or other estimates of the integral can be used, if desired. The relaxation program was written using Symantec's Think Pascal software and run on a Macintosh LCII and a Macintosh Centris 650.

[1] R. W. Chabay and B. A. Sherwood, *Electric and Magnetic Interactions* (Wiley, New York, 1995), esp. Chap. 6.

[2] R. P. Feynman, R. B. Leighton, and M. Sands, *The Feynman Lectures on Physics* (Addison-Wesley, Redwood City, CA, 1989).

[3] P. Fishbane, S. Gasiorowicz, and S. T. Thornton, *Physics for Scientists and Engineers* (Prentice-Hall, Englewood Cliffs, NJ, 1993).

[4] D. C. Giancoli, *Physics for Scientists and Engineers* (Prentice-Hall, Englewood Cliffs, NJ, 1988).

[5] J. W. Kane and M. M. Sternheim, *Physics* (Wiley, New York, 1988), 3rd ed.

[6] F. Miller and D. Schroeer, *College Physics* (Harcourt Brace Jovanovich, San Diego, 1987), 6th ed.

[7] H. C. Ohanian, *Physics* (Norton, New York, 1989), 2nd ed.

[8] E. M. Purcell, *Electricity and Magnetism*, Berkeley Physics Course, Vol. 2 (McGraw-Hill, New York, 1985), 2nd ed.

[9]R. Resnick, D. Halliday, and K. S. Krane, *Physics for Students in Science and Engineering* (Wiley, New York, 1992), 4th ed.
[10]P. A. Tipler, *Physics for Scientists and Engineers* (Worth, New York, 1990), 3rd ed.
[11]O. D. Jefimenko, *Electricity and Magnetism* (Appleton-Century-Crofts, New York, 1966) [2nd ed., Electret Scientific Co., Star City, WV, 1989].
[12]P. Lorrain, D. Corson, and F. Lorrain, *Electromagnetic Fields and Waves* (Freeman, New York, 1988), 3rd ed.
[13]D. J. Griffiths, *Introduction to Electrodynamics* (Prentice-Hall, Englewood Cliffs, NJ, 1989), 2nd ed.
[14]J. R. Reitz, F. J. Milford, and R. W. Christy, *Foundations of Electromagnetic Theory* (Addison-Wesley, Reading, MA, 1993), 4th ed.
[15]J. D. Jackson, *Classical Electrodynamics* (Wiley, New York, 1975), 2nd ed.
[16]L. D. Landau, E. M. Lifshitz, and L. P. Pitaevskii, *Electrodynamics of Continuous Media* (Pergamon, Oxford, 1984), 2nd ed.
[17]W. K. H. Panofsky and M. Phillips, *Classical Electricity and Magnetism* (McGraw-Hill, New York, 1962) 2nd ed.
[18]W. R. Smythe, *Static and Dynamic Electricity* (McGraw-Hill, New York, 1968), 3rd ed.
[19]C. Schaeffer, *Einführung in die theoretische Physik* (Walter de Gruyter, Berlin, 1932), Vol. 3, part 1, pp. 175–184.
[20]A. Marcus, "The electric field associated with a steady current in long cylindrical conductor," Am. J. Phys. **9**, 225–226 (1941).
[21]A. Sommerfeld, *Electrodynamics*, Lectures on Theoretical Physics, Vol. III (Academic, New York, 1952), pp. 125–130.
[22]O. Jefimenko, "Demonstration of the electric fields of current-carrying conductors," Am. J. Phys. **30**, 19–21 (1962).
[23]W. G. V. Rosser, "What makes an electric current flow," Am. J. Phys. **31**, 884–885 (1963).
[24]B. R. Russell, "Surface charge on conductors carrying steady currents," Am. J. Phys. **36**, 527–529 (1968).
[25]W. G. V. Rosser, "Magnitudes of surface charge distributions associated with current electric flow," Am. J. Phys. **38**, 265–266 (1970).
[26]S. Parker, "Electrostatics and current flow," Am. J. Phys. **38**, 720–723 (1970).
[27]M. A. Heald, "Electric fields and charges in elementary circuits," Am. J. Phys. **52**, 522–526 (1984).
[28]R. N. Varney and L. H. Fisher, "Electric fields associated with stationary currents," Am. J. Phys. **52**, 1097–1099 (1984).
[29]W. R. Moreau, S. G. Ryan, S. J. Beuzenberg, and R. W. G. Syme, "Charge density in circuits," Am. J. Phys. **53**, 552–553 (1985).
[30]J. M. Aguirregabiria, A. Hernandez, and M. Rivas, "An example of surface charge distribution on conductors carrying steady currents," Am. J. Phys. **60**, 138–141 (1992). See also J. M. Aguirregabiria, A. Hernandez, and M. Rivas, "Surface charges and energy flow in a ring rotating in a magnetic field," to be published in Am. J. Phys.
[31]The first sentence of the italicized statement on p. 211 of Ref. 1 is a clear expression of these global aspects. The second sentence is, however, misleading in its implication that bends in the wires are the only cause of "counter-intuitive" surface charge densities.
[32]The choice of a straight conductor precludes illustration of surface charges present to "guide" the current around corners. A generalization of Heald's circuit (Ref. 27) to a circular annulus (cylinder) of finite thickness has an intuitively expected difference in charge density on the inner and outer surfaces to maintain the azimuthal current flow within the annulus.
[33]J. N. Marx and D. R. Nygren, "The Time-Projection Chamber," Phys. Today **31** (10), 46–53 (October 1978).
[34]The linear vanishing of the charge density at $z=0$ and $z=L$ is an artifact of the specific termination in flat plates at right angles to the column. See Ref. 15, p. 77.
[35]See Ref. 15, p. 77.
[36]A generalization of the second form given in Problem 3.21, p. 134 of Ref. 15.
[37]To express the charge densities in SI formulas, multiply the right-hand sides by $4\pi\epsilon_0$. The units of charge density are then $\epsilon_0 V/L$. Charges are most conveniently expressed in units of Va ($4\pi\epsilon_0 Va$ in SI notation) and capacitances in units of a ($4\pi\epsilon_0 a$ in SI notation). Numerically, 1 cm of capacitance=1.11265 pF≈1 pF.
[38]L. B. W. Jolley, *Summation of Series* (Dover, New York, 1961), 2nd rev. ed., p. 96, Nos. 508 and 509.

A graphical representation of the Dirac algebra

David M. Goodmanson
2725 68th Avenue S.E., Mercer Island, Washington 98040

(Received 11 September 1995; accepted 16 October 1995)

The elements of the Dirac algebra are represented by sixteen 4×4 gamma matrices, each pair of which either commute or anticommute. This paper demonstrates a correspondence between the gamma matrices and the complete graph on six points, a correspondence that provides a visual picture of the structure of the Dirac algebra. The graph shows all commutation and anticommutation relations, and can be used to illustrate the structure of subalgebras and equivalence classes and the effect of similarity transformations. Since gamma matrices are the direct products of two Pauli spin matrices, they provide an appropriate way to describe a system of two spin-1/2 particles. Such multiparticle spin states are intimately connected with the theorems of John Bell. The graph is helpful in analyzing an important example of the Bell–Kochen–Specker theorem.

I. INTRODUCTION

In this paper I wish to point out a useful isomorphism between the Dirac algebra and the complete graph on six points. The isomorphism provides a picture of the algebra and illustrates its underlying structure. I feel that a visual representation of the Dirac algebra is of great benefit, because it can provide an additional insight that is not easily expressed with words or equations. And the diagram also has a practical side. It can be a fast and convenient way to find the right gamma matrix in a given situation.

Gamma matrices can be constructed as direct products of

